WATER RESOURCES RESEARCH, VOL. 16, NO. 4, PAGES 643–650, AUGUST 1980

Some Effects of Linearizing the Unsaturated Soil Moisture Transfer Diffusivity Model

T. V. HROMADKA II AND G. L. GUYMON

School of Engineering, University of California, Irvine, California 92717

Five methods are evaluated for estimating the nonlinear diffusivity coefficient in a finite element Crank-Nicolson analog of the diffusivity model for moisture transfer in an unsaturated horizontal homogeneous soil column. The Galerkin technique is utilized for the quasi-linear spatial discretization problem, and the commonly used Crank-Nicolson time advancement method is used with a diffusivity coefficient update method based upon (1) a constant diffusivity coefficient for all space and time and (2) a quasi-constant diffusivity coefficient within each element during a Crank-Nicolson time step. In the case of constant diffusivity coefficient problems a modified capacitance matrix scheme significantly improves results over the standard finite element capacitance matrix. For nonlinear problems, five methods of estimating quasi-constant soil water diffusivity equivalents were evaluated. These are (1) a straight line average using element endpoint water content in a diffusivity function, (2) an integration of the diffusivity constant over each element, (3) an inverse diffusivity function integration over each element, (4) an evaluation of the diffusivity coefficient as the mean parabolic value over a specified subdomain of each element, and (5) an evaluation of the diffusivity coefficient for each element at one half of the Crank-Nicolson time step, using method 4. Both the modified and unmodified finite element capacitance matrices were used for each method considered. The unmodified finite element capacitance matrices based upon values of diffusivity coefficients evaluated as the mean parabolic value of the state variable gave the superior results.

INTRODUCTION

Finite element techniques have been applied to numerical solution of moisture transfer in soils by a number of investigators [e.g., *Bruch and Zyvoloski*, 1974; *Neuman et al.*, 1975]. A substantial amount of work has been done on the efficiency and accuracy of finite element Galerkin techniques [*Douglas and Dupont*, 1970; *Price et al.*, 1968; *Hayhoe*, 1978]. In the case of moisture transfer in unsaturated soils the flow equation is nonlinear, and normally, to apply the finite element method, the governing partial differential equation is linearized. Few have investigated the effects of finite time step advancement schemes and the linearization of the flow equation on the numerical solutions based upon the finite element method. The objective of this paper is to study the effects of one such linearizing approach.

Horizontal infiltration of water into a homogeneous soil column of length L is described by the nonlinear partial differential equation

$$\frac{\partial}{\partial x}\left[D(\theta)\frac{\partial\theta}{\partial x}\right]=\frac{\partial\theta}{\partial t} \tag{1}$$

where θ is the dimensionless soil volumetric water content, x is the horizontal spatial coordinate, t is time, $D(\theta)$ is the soil water diffusivity, and appropriate initial and boundary conditions are required.

The finite element approach used to solve (1) is the Galerkin version of the weighted residual process [*Desai*, 1979]. The solution domain is discretized into the union of n finite elements by

$$L=\bigcup_{i=1}^{n}L_i \tag{2}$$

The water content is utilized as the state variable and is approximated within each finite element by

$$\theta(x)=\sum N_j\theta_j \tag{3}$$

Paper number 80W0465.
0043-1397/80/080W-0465$01.00

where N_j are the appropriate linearly independent shape functions and θ_j are the state variable values at element nodal points designated by the general summation index j. The Galerkin technique utilizes the set of shape functions as the weighting functions, which indicates that the corresponding finite element representation for the infiltration process is

$$\int\left\{\frac{\partial}{\partial x}\left[D(\theta)\frac{\partial\theta}{\partial x}\right]-\frac{\partial\theta}{\partial t}\right\}N_j\,dx=0 \tag{4}$$

Integration by parts expands (4) into the form

$$\sum_{i=1}^{n}\left\{D(\theta)\frac{\partial\theta}{\partial x}N_j\bigg|_{S_i}-\int_{L_i}\left[D(\theta)\frac{\partial\theta}{\partial x}\frac{\partial N_j}{\partial x}+N_j\frac{\partial\theta}{\partial t}\right]dx\right\}=0 \tag{5}$$

where S_i are the external endpoints of the one-dimensional finite element L_i. The first term within the braces sums to zero for interior elements and also satsifies specified or flux-type boundary conditions of the problem for exterior boundaries. The remaining integral term is solved by substituting the appropriate element approximations and shape functions into the integrand and solving by numerical integration. The nonlinear nature of the partial differential equation, however, generally introduces difficulties in integrating (5). A convenient linearizing approach is to assume the diffusivity function to be constant within each finite element during a finite time interval Δt [e.g., *Guymon and Luthin*, 1974]. By assuming the diffusivity function to be constant within each finite element, error is introduced into the numerical solution. Additional errors are introduced because of the spatial and time discretizations of partial derivatives in the governing flow equation.

The Crank-Nicolson time advancement approximation has been widely used [*Hayhoe*, 1978; *Desai*, 1979] to solve the time derivative of (5). The time derivative could also be approximated by the Galerkin technique [*Bruch and Zyvoloski*, 1974]; however, it does not appear to be advantageous [*Yoon and

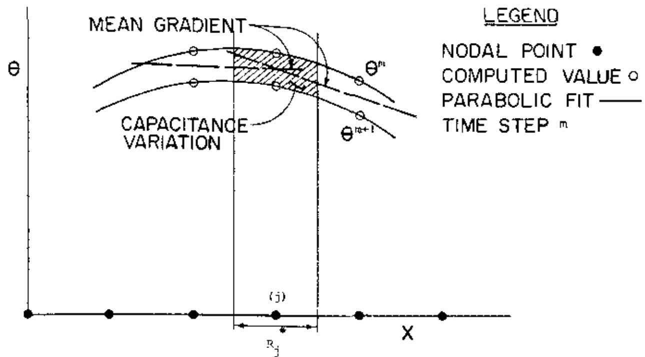

Fig. 1. Nodal domain of soil water mass balance.

Yeh, 1975]. The Crank-Nicolson formulation reduces (5), where values of soil water diffusivity are assumed constant within each finite element, into a system of linear equations expressed in matrix form as

$$\left\{\mathbf{P} + \frac{\Delta t}{2}\mathbf{S}\right\}\theta^{m+1} = \left\{\mathbf{P} - \frac{\Delta t}{2}\mathbf{S}\right\}\theta^{m} \tag{6}$$

where **P** is a symmetrical capacitance matrix and is a function of element nodal global coordinates, S is a symmetrical stiffness matrix and is a function of element nodal global coordinates and constant finite element diffusivity coefficients (during time step Δt), and Δt is the finite time step increment where θ^k is a vector representing θ at each node and time step k.

The objective of this paper is to evaluate the Crank-Nicolson method as applied to (5) and to examine some of the methods of determining quasi-constant values of diffusivity utilized in the linearized matrix formulation of (6). First, (1) and (6) will be analyzed with respect to the idealized assumption of a constant diffusivity throughout the soil column for time $t \geq 0$. Second, the model of a variable diffusivity function as quasi-constant within each finite element during a Crank-Nicolson time step Δt, but variable between elements, will be analyzed. The horizontal infiltration of water into an air dry soil column as described by *Hayhoe* [1978] is utilized for numerical study purposes. Graphical illustrations of numerical results compared to the exact solution [*Philip and Knight,* 1974] are provided to indicate the relative numerical accuracy between the various methods considered for determining quasi-constant values of soil water diffusivity.

CONSTANT SOIL WATER DIFFUSIVITY

In this section, one-dimensional horizontal soil water transfer is defined by

$$\frac{\partial}{\partial x} D(\theta) \frac{\partial \theta}{\partial x} = \frac{\partial \theta}{\partial t} \qquad \{x: 0 \leq x \leq L\}$$

$$D(\theta) = D \qquad D \text{ constant} \tag{7}$$

with initial and boundary conditions

$$\theta(x, t) = \theta_0 \qquad t = 0$$

$$\theta(\text{o}, t) = \theta(L, t) = \theta_b \qquad t > 0 \tag{8}$$

$$0 \leq \theta_b < \theta_0 < \text{soil porosity}$$

This specialized problem can be normalized into the form

$$\frac{\partial^2 \theta}{\partial x^2} = \frac{\partial \theta}{\partial t} \qquad x: \{0 \leq x \leq 1\} \tag{9}$$

with initial and boundary conditions

$$\theta(x, t) = 1 \qquad t = 0$$

$$\theta(\text{o}, t) = \theta(1, t) = 0 \qquad t > 0 \tag{10}$$

For a linear polynomial shape function the element matrices determined from (5) for a Galerkin approximation of (9) are given by

$$\hat{\mathbf{S}}\begin{Bmatrix}\theta_i\\ \theta_j\end{Bmatrix} + \hat{\mathbf{P}}\begin{Bmatrix}\dot\theta_i\\ \dot\theta_j\end{Bmatrix} = \frac{1}{l_i}\begin{bmatrix}1 & -1\\ -1 & 1\end{bmatrix}\begin{Bmatrix}\theta_i\\ \theta_j\end{Bmatrix} + \frac{l_i}{6}\begin{bmatrix}2 & 1\\ 1 & 2\end{bmatrix}\begin{Bmatrix}\dot\theta_i\\ \dot\theta_j\end{Bmatrix} \tag{11}$$

where $\hat{\mathbf{S}}$ and $\hat{\mathbf{P}}$ are element stiffness and capacitance matrices, respectively, and (θ_i, θ_j) and $(\dot\theta_i, \dot\theta_j)$ refer to the element nodal and the time derivative of nodal moisture content values, respectively, for an element of length l_i.

For discussion purposes, let the domain L be discretized into disjoint L_i of equal dimension such that $l_i = l$ for every i. Then for an interior nodal point, simultaneous solution of (6) and (11) gives

$$\frac{1}{2l}[(\theta_k - \theta_j)^{m+1} - (\theta_j - \theta_i)^{m+1} + (\theta_k - \theta_j)^m - (\theta_j - \theta_i)^m]$$

$$= \frac{l}{6\Delta t}[(\theta_i + 4\theta_j + \theta_k)^{m+1} - (\theta_i + 4\theta_j + \theta_k)^m] \tag{12}$$

where the nodal value θ_j is interior to nodal values (θ_i, θ_k) and the superscripts indicate successive time step values.

The Crank-Nicolson time step advancement routine defines a new domain R_j for each nodal point θ_j (see Figure 1) such that

$$R_j \equiv \left\{x: \ x_j - \frac{l}{2} \leq x \leq x_j + \frac{l}{2}\right\} \tag{13}$$

wherein (12) approximates the integrated version of (9) on R_j

$$\left.\frac{\partial \theta}{\partial x}\right|_{x_j-(l/2)}^{x_j+(l/2)} = \frac{\partial}{\partial t}\int_{x_j-(l/2)}^{x_j+(l/2)} \theta \, dx = \frac{\partial}{\partial t}\int_{R_j} \theta \, dx \tag{14}$$

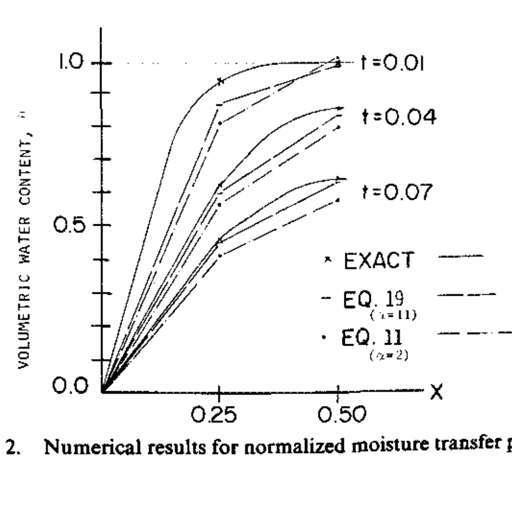

Fig. 2. Numerical results for normalized moisture transfer problem.

TABLE 1. Simulated Results for Equations (9) and (10) With $(\Delta x, \Delta t) = (0.25, 0.01)$ for Constant Diffusivity

Time	Unmodified Capacitance Matrix ($\alpha = 2$)		Modified Capacitance Matrix ($\alpha = 11$)		Analytic Solution	
	$x = 0.25$	$x = 0.50$	$x = 0.25$	$x = 0.50$	$x = 0.25$	$x = 0.50$
0.01	0.802	1.041	0.851	0.989	0.923	0.999
0.02	0.701	0.970	0.743	0.941	0.789	0.975
0.03	0.627	0.881	0.660	0.876	0.690	0.918
0.04	0.564	0.796	0.592	0.807	0.615	0.846
0.05	0.508	0.718	0.533	0.739	0.553	0.772
0.06	0.457	0.647	0.482	0.674	0.499	0.702
0.07	0.412	0.583	0.437	0.614	0.452	0.637
0.08	0.372	0.525	0.396	0.558	0.409	0.578
0.09	0.335	0.474	0.360	0.508	0.370	0.524
0.10	0.302	0.427	0.327	0.461	0.336	0.474
0.11	0.272	0.385	0.297	0.419	0.304	0.430
0.12	0.245	0.347	0.269	0.381	0.275	0.390
0.13	0.221	0.312	0.245	0.346	0.250	0.353
0.14	0.119	0.282	0.222	0.314	0.226	0.320
0.15	0.179	0.254	0.202	0.285	0.205	0.290
0.16	0.162	0.229	0.183	0.259	0.186	0.262
0.17	0.146	0.206	0.166	0.235	0.168	0.238
0.18	0.131	0.186	0.151	0.214	0.152	0.215
0.19	0.118	0.167	0.137	0.194	0.138	0.195
0.20	0.107	0.151	0.125	0.176	0.125	0.177

where x_j is the global coordinate of nodal point j.

However, the capacitance term of (12) represents the difference between the mean parabolic value of the state variable θ within the domain

$$\{x: x_j - l \leq x \leq x_j + l\}$$

at time steps m and $m + 1$, and the transport (stiffness) term is the time-averaged spatial gradient (at time step $m + 1/2$) of the state variable at the endpoints of R_j. Thus the element capacitance matrix may be modified to approximate the integration of water content on R_j:

$$\int_{R_j} \theta \, dx \equiv \int_{x_j-(l/2)}^{x_j+(l/2)} \eta(\theta) dx \tag{15}$$

where $\eta(\theta)$ is the appropriate set of state variable approximation functions. For a set of linear shape function approximations on R_j,

$$\int_{R_j} \theta \, dx = \frac{l}{8} (\theta_i + 6\theta_j + \theta_k) \tag{16}$$

For a set of second-order polynomial shape function approximations,

$$\int_{R_j} \theta \, dx \approx \frac{l}{24} (\theta_i + 22\theta_j + \theta_k) \tag{17}$$

In (17) an approximation is designated due to shape function contributions within R_j from neighboring finite elements. In (16) the relation is precise. Also, the spatial gradient of water content evaluated at the boundaries of R_j as given in (12) applies to both (16) and (17).

The modified finite element capacitance matrix corresponding to (16) is

$$\hat{\mathbf{P}}(3) = \frac{l}{8} \begin{bmatrix} 3 & 1 \\ 1 & 3 \end{bmatrix} \tag{18}$$

Likewise, the element capacitance matrix corresponding to (17) is

$$\hat{\mathbf{P}}(11) = \frac{l}{24} \begin{bmatrix} 11 & 1 \\ 1 & 11 \end{bmatrix} \tag{19}$$

where in (18) and (19), $\hat{\mathbf{P}}(\alpha)$ is defined by

$$\hat{\mathbf{P}}(\alpha) = \frac{l}{2(\alpha + 1)} \begin{bmatrix} \alpha & 1 \\ 1 & \alpha \end{bmatrix} \tag{20}$$

From (20) the finite element capacitance matrix of (11) is given by $\alpha = 2$. Additionally, a standard finite difference approximation results for the element capacitance matrix by

$$\lim_{\alpha \to \infty} \hat{\mathbf{P}}(\alpha) = \frac{l}{2} \begin{bmatrix} 1 & 0 \\ 0 & 1 \end{bmatrix} \tag{21}$$

Using (20), the Crank-Nicolson finite element approximation of (6) can be expressed as a function of the element capacitance matrix formulation by the global matrix system

$$A(\alpha) \equiv \left\{ \left[\mathbf{P}(\alpha) + \frac{\Delta t}{2} \mathbf{S} \right] \theta^{m+1} = \left[\mathbf{P}(\alpha) - \frac{\Delta t}{2} \mathbf{S} \right] \theta^m \right\} \tag{22}$$

where $A(\alpha)$ refers to the numerical model approximation of (9) and (10) as a function of α.

A computer program based on (22) was prepared to model (9) and (10) for various values of α. The analytical series solution to (9) and (10) is given by a modified form of the solution presented by *Myers* [1971]:

$$\theta(x, t) = \frac{4}{\pi} [(\sin \pi x) e^{-\pi^2 t} + \tfrac{1}{3} (\sin 3\pi x) e^{-9\pi^2 t} + \cdots] \tag{23}$$

TABLE 2. Simulated Results for Equations (9) and (10) With (Δx, Δt) = (0.05, 0.01) for Constant Diffusivity

Time	Unmodified Capacitance Matrix ($\alpha = 2$)		Modified Capacitance Matrix ($\alpha = 11$)		Analytic Solution	
	$x = 0.25$	$x = 0.50$	$x = 0.25$	$x = 0.50$	$x = 0.25$	$x = 0.50$
0.01	0.941	0.997	0.938	0.996	0.923	0.999
0.02	0.788	0.977	0.790	0.975	0.789	0.975
0.03	0.673	0.924	0.679	0.922	0.690	0.918
0.04	0.618	0.847	0.616	0.847	0.615	0.846
0.05	0.546	0.771	0.549	0.772	0.553	0.772
0.06	0.498	0.701	0.499	0.702	0.499	0.702
0.07	0.450	0.635	0.451	0.636	0.452	0.637
0.08	0.406	0.575	0.408	0.577	0.409	0.578
0.09	0.370	0.521	0.370	0.523	0.370	0.524
0.10	0.332	0.472	0.334	0.474	0.336	0.474
0.11	0.304	0.428	0.304	0.429	0.304	0.430
0.12	0.273	0.387	0.275	0.389	0.275	0.390
0.13	0.249	0.351	0.249	0.352	0.250	0.353
0.14	0.224	0.318	0.226	0.319	0.226	0.320
0.15	0.204	0.288	0.205	0.289	0.205	0.290
0.16	0.184	0.261	0.185	0.262	0.186	0.262
0.17	0.167	0.236	0.168	0.237	0.168	0.238
0.18	0.151	0.214	0.152	0.215	0.152	0.215
0.19	0.137	0.194	0.138	0.195	0.138	0.195
0.20	0.124	0.176	0.125	0.177	0.125	0.177

Equations (9) and (10) were first modeled by discretizing the one-dimensional domain into four linear finite elements of length 0.25 and using a Crank-Nicolson time step of Δt = 0.01. The symmetric simulated results at x equal 0.5 for element capacitance matrix alternatives given by $\alpha = (2, 11)$ and the analytic solution, (23), are shown in Figure 2 for times t = 0.01, 0.04, and 0.07.

From Figure 2 the modified capacitance matrix ($\alpha = 11$) improves computational accuracy over those results given by the finite element approach ($\alpha = 2$). Table 1 includes the simulated results from both the modified ($\alpha = 11$) and unmodified ($\alpha = 2$) capacitance matrix formulations and the analytic solution for $0 < t \leq 0.20$. Comparison of simulated results to the analytic solution indicates an increase in accuracy when utilizing the modified capacitance matrix approach. Table 2 includes the simulated results from both the modified and unmodified capacitance matrix approaches for solution of (9) and (10) with $\Delta x = 0.05$ and with time step $\Delta t = 0.01$. Again, increased accuracy is achieved when modifying the capacitance element matrix according to (19).

In order to evaluate better the numerical model obtained by using (18) and (19) for the element capacitance matrix in (6), $A(\alpha)$ was solved for the finite element approach ($\alpha = 2$), the modified finite element approaches ($\alpha = 3, 11$), and an approximation for the standard finite difference method ($\alpha = 1000$). Again, a spatial discretization of $\Delta x = 0.25$ and a time step of $\Delta t = 0.01$ was used.

To compare numerical methods, three error tests were used. These are defined as follows:

$$RMS(a) \equiv \frac{1}{a} \sum_{i=1}^{a} \left[\frac{(\epsilon_i - e_i)^2}{\epsilon_i} \right]^{1/2} \tag{24}$$

$$CRE(a) = \frac{1}{a} \sum_{i=1}^{a} \frac{|\epsilon_i - e_i|}{\epsilon_i} \tag{25}$$

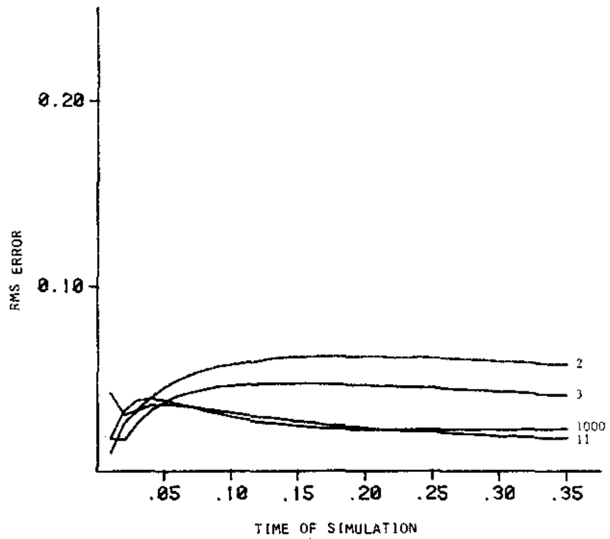

Fig. 3. Cumulative RMS error for normalized moisture transport problem.

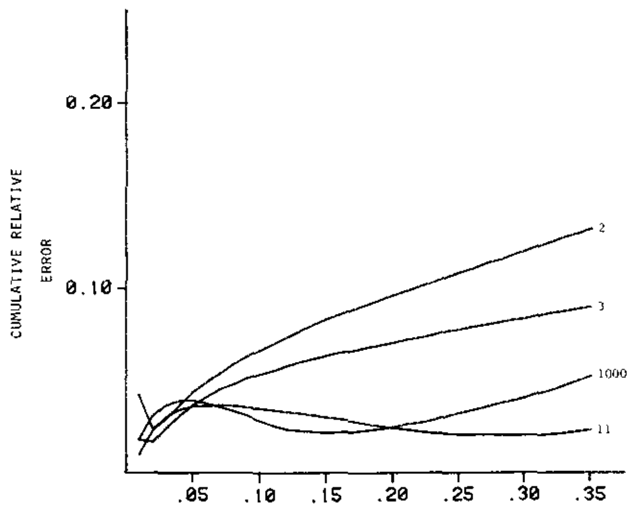

Fig. 4. Cumulative relative error for normalized moisture transport problem.

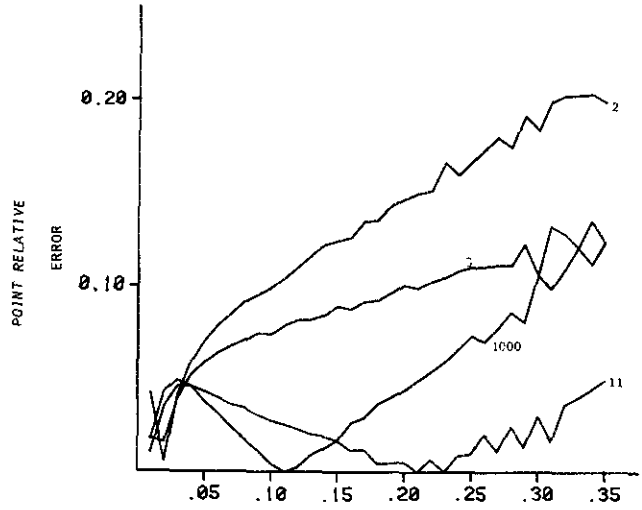

Fig. 5. Point relative error for normalized moisture transport problem.

$$RE(a) = \frac{|\epsilon_i - e_i|}{\epsilon_i} \quad (26)$$

where $RMS(a)$ represents a modified form of a root-mean-square error averaged over duration $0 \leq t \leq a\Delta t$, $CRE(a)$ is an averaged relative error over duration $0 \leq t \leq a\Delta t$, $RE(a)$ is the relative error at time $t = a\Delta t$, ϵ_i and e_i are the analytic value from (23) and computed value, respectively, at time $t = i\Delta t$, and 'a' is an integer.

Figures 3–5 show plots of the tested error functions versus simulation time for the $RMS(a)$, $CRE(a)$, and $RE(a)$ functions, respectively. Total simulation duration used was $0 \leq t \leq 0.35$. From the results the modified finite element formulation using (19) provides the best overall accuracy in each of the three tests for the test problem.

A second model analysis was performed by determining a best integer α as a function of simulation duration for each of the three tests. That is,

$$\alpha_{RMS}^{(a)} \equiv \min_{\alpha} RMS(a) \quad (27)$$

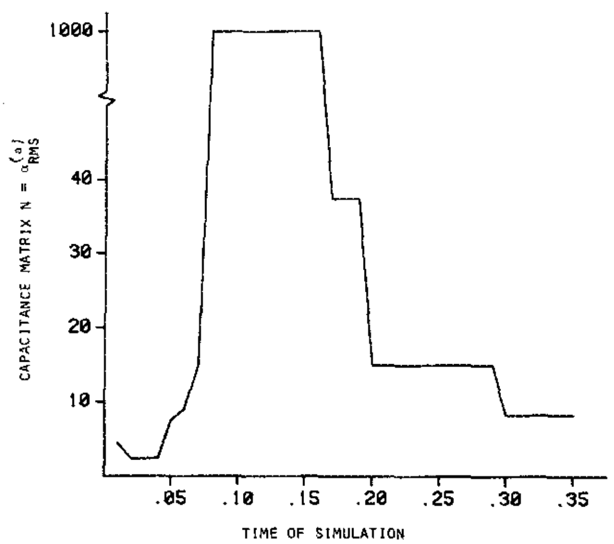

Fig. 6. Optimum capacitance matrix n for cumulative RMS error of normalized moisture transport problem.

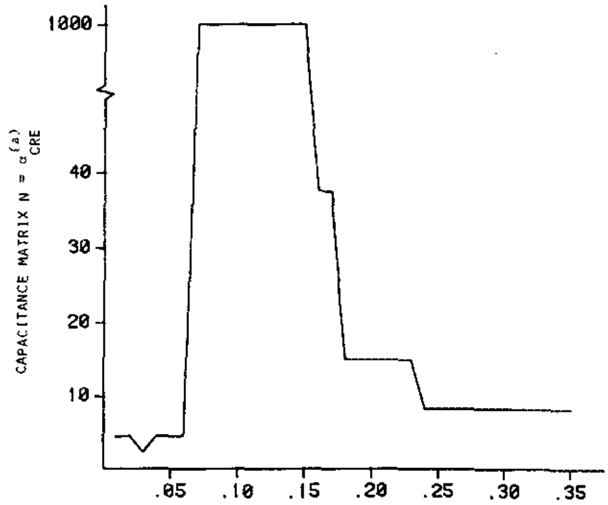

Fig. 7. Optimum capacitance matrix n for cumulative relative error of normalized moisture transport problem.

$$\alpha_{CRE}^{(a)} \equiv \min_{\alpha} CRE(a) \quad (28)$$

$$\alpha_{RE}^{(a)} \equiv \min_{\alpha} RE(a) \quad (29)$$

Values of α were considered where α was set to (1, 2, 3, 4, 6, 10, 11, 12, 15, 20, 50, 1000).

Figures 6–8 give plots for (27), (28), and (29) as a function of simulation duration $a\Delta t$. This analysis indicates that although the standard finite difference method provides a temporary higher degree of accuracy, the modified finite element formulations give the better overall approximations to (9) and (10).

VARIABLE SOIL WATER DIFFUSIVITY

This section examines the computational accuracy of the finite element method when using the Crank-Nicolson time advancement method for soil moisture transfer problems where the diffusivity coefficient is a function of the water content. As in the previous section, a linear polynomial shape function is

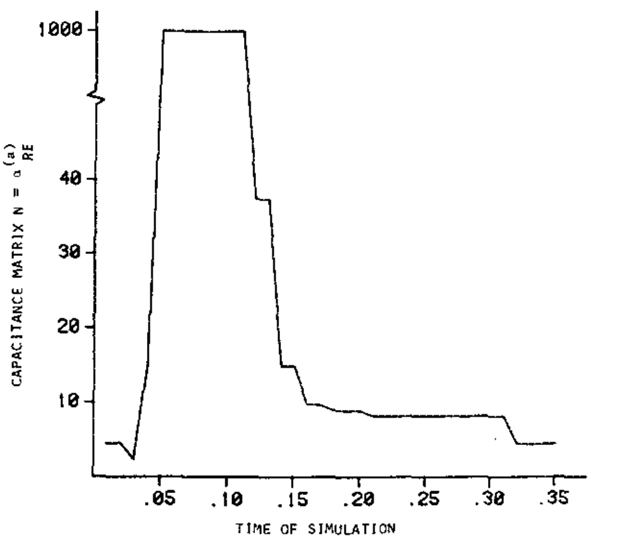

Fig. 8. Optimum capacitance matrix n for point relative error of normalized moisture transport problem.

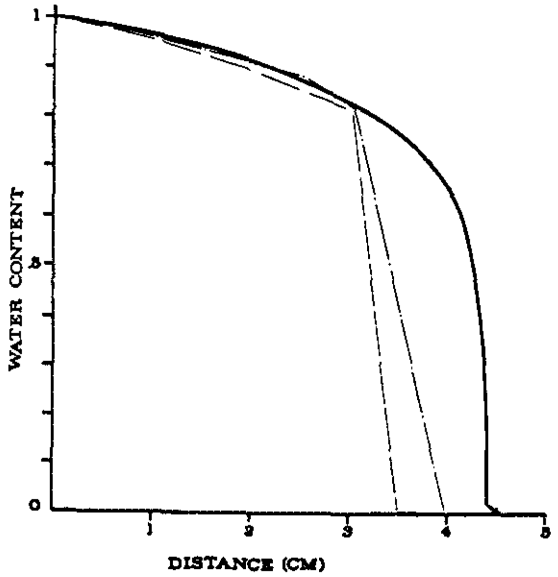

Fig. 9. Results from diffusivity coefficient computed from (32). Dashed line is unmodified matrix; single-dot-dashed line is modified matrix formulation; solid line is exact solution.

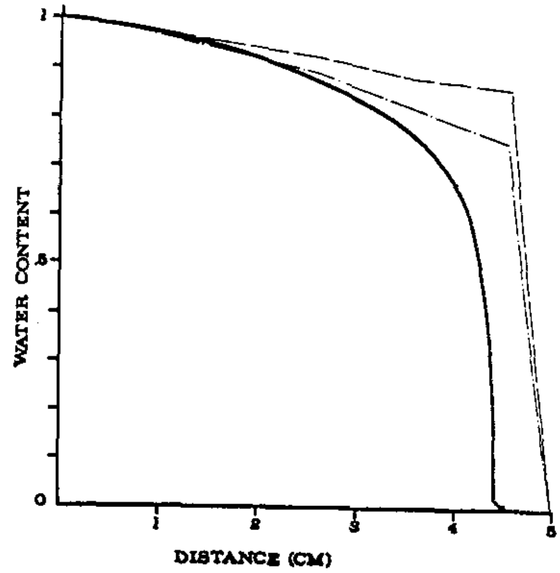

Fig. 11. Results from diffusivity coefficient computed from (34). Dashed line is unmodified matrix; single-dot-dashed line is modified matrix formulation; solid line is exact solution.

used; additionally, the diffusivity coefficient is assumed quasi-constant within each finite element. Horizontal infiltration of water into an air dry horizontal soil column is utilized as a test problem [*Hayhoe*, 1978]. The analytic value of soil water diffusivity for Hanford sandy loam [*Reichardt et al.*, 1972] was selected in order to provide a sharp wetting front through the soil column, causing the numerical analysis of moisture flow in the soil to be difficult. The quasi-analytic solution advanced by *Philip and Knight* [1974] and utilized by *Hayhoe* [1978] was used for this study.

Equation (1) was solved subject to the initial condition

$$\theta(x, t) = 0 \qquad t = 0 \qquad 0 \le x \le L \tag{30}$$

and the boundary conditions

$$\theta(0, t) = 1 \qquad \theta(L, t) = 0 \qquad t > 0 \tag{31}$$

where the soil water diffusivity (in square centimeters per minute) is given by

$$D(\theta) = 0.9 \times 10^{-3} \exp(8.36\theta) \qquad \theta > 0$$

$$D(\theta) = 0.9 \times 10^{-3} \qquad \theta = 0$$

and θ is the dimensionless volumetric water content. Constant values of soil water diffusivity were assumed in each finite element during a time step Δt. After computation of water content, $D(\theta)$ is reevaluated for each finite element, and the global matrix system (6) is adjusted accordingly.

Five techniques were used for computing a constant valued equivalent $D_i(\theta)$ for a variable diffusivity function in each finite element, namely,

$$D_i(\theta) = D[(\theta_i + \theta_{i+1})/2] \tag{32}$$

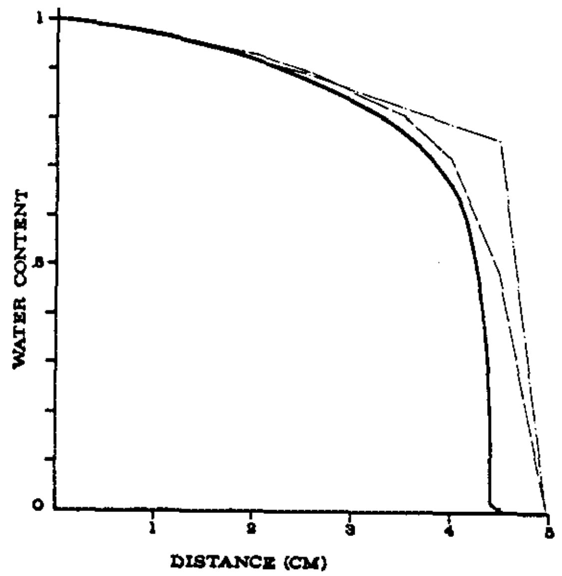

Fig. 10. Results from diffusivity coefficient computed from (33). Dashed line is unmodified matrix; single-dot-dashed line is modified matrix formulation; solid line is exact solution.

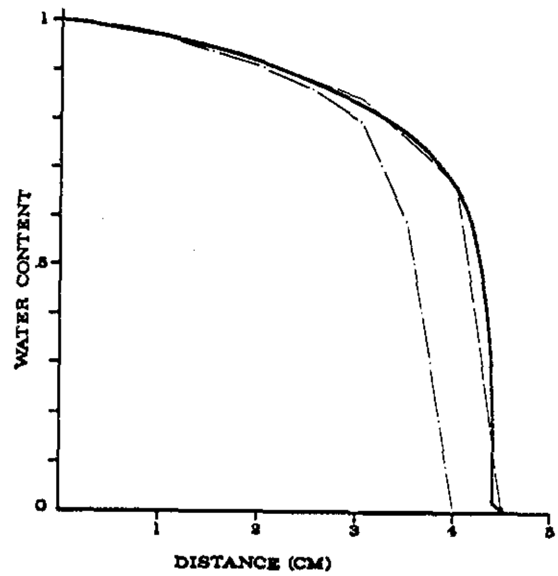

Fig. 12. Results from diffusivity coefficient computed from (35). Dashed line is unmodified matrix; single-dot-dashed line is modified matrix formulation; solid line is exact solution.

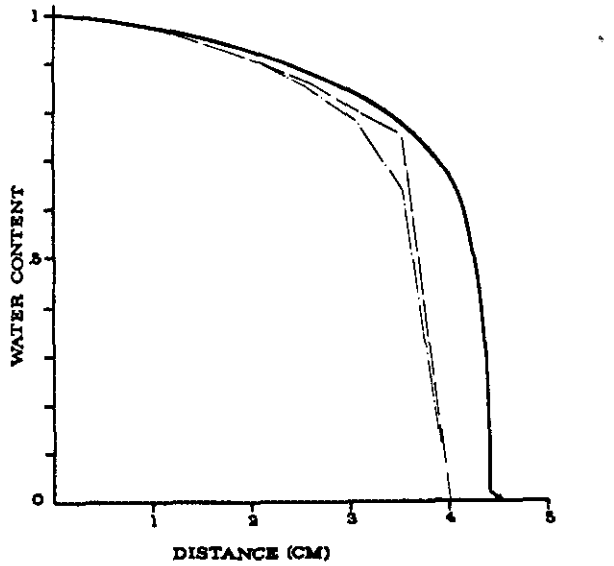

Fig. 13. Results from diffusivity coefficient computed from (37). Dashed line is unmodified matrix; single-dot-dashed line is modified matrix formulation; solid line is exact solution.

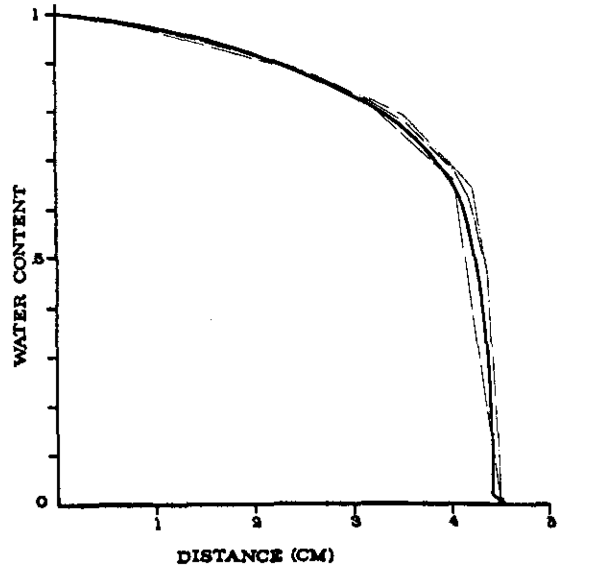

Fig. 15. Results from unmodified matrix formulation (diffusivity coefficients from (35)) for $\Delta x = 0.125$ cm; (single-dot dashed line), $\Delta x = 0.250$ (double-dot-dashed line); $\Delta x = 0.50$ (dashed line).

$$D_i(\theta) = \frac{1}{l_i}\int_{x_i}^{x_{i+1}} D(\theta(x))\, dx \tag{33}$$

$$D_i^{-1}(\theta) = \frac{1}{l_i}\int_{x_i}^{x_{i+1}} D^{-1}(\theta(x))\, dx \tag{34}$$

where $D_i(\theta)$ is assumed constant within finite element number i and (θ_i, θ_{i+1}) are the nodal values of soil water content for element i.

The fourth technique used for computing quasi-constant values of soil water diffusivity involves evaluating the diffusivity function at the mean parabolic value of the state variable at the endpoints of R_j (Figure 1). That is, for P_k equal to the parabolic polynomial fitted to nodal values $(\theta_{k-1}, \theta_k, \theta_{k+1})$ for $k = i, i+1$, then for interior finite elements, method four sets

$$D_i(\theta) = D\left\{\tfrac{1}{2}\left[P_i\left(x(\theta_i) + \frac{l_i}{2}\right) + P_{i+1}\left(x(\theta_i) + \frac{l_i}{2}\right)\right]\right\} \tag{35}$$

or

$$D_i(\theta) = D\left\{\frac{1}{16}\left[-\theta_{i-1} + 9\theta_i + 9\theta_{i+1} - \theta_{i+2}\right]\right\} \tag{36}$$

Finally, the fifth technique examined is the utilization of (35) in the evaluation of $D_i(\theta)$ at time step $(m + \frac{1}{2})$. That is,

$$D_i(\theta) = \tfrac{1}{2}[\hat{D}_i^m(\theta) + \hat{D}_i^{m+1}(\theta)] \tag{37}$$

where $\hat{D}_i^k(\theta)$ is the value of soil water diffusivity evaluated at the mean parabolic value of the state variable per (35) and (36) at time steps k.

Both the modified ($\alpha = 11$) and unmodified ($\alpha = 2$) capacitance matrix approaches were utilized in evaluating the computational accuracy of each of the five methods studied in determining quasi-constant values for element soil water diffusivity.

The soil moisture profile at time $t = 16.5$ min was selected as the study case in order to compare computer simulations to the results reported by *Hayhoe* [1978]. For evaluation of the integrals in (33) and (34) a linear variation of soil water content was assumed between element nodal points (linear polynomial shape function). A constant element size of $\Delta x = 0.50$ cm and a time step size of $\Delta t = 0.1$ min was employed.

Figures 9–13 compare the simulated results for (1), (30), and (31) between the modified and unmodified capacitance matrix approaches for each of the five constant diffusivity coefficient computation schemes. From the results the modified capacitance matrix approach improves computational accuracy only for values of constant diffusivity determined by (32) and (34). Of significance are the results shown in Figure 12 which display the simulated results of using the finite element capacitance matrix ($\alpha = 2$) and constant finite element diffu-

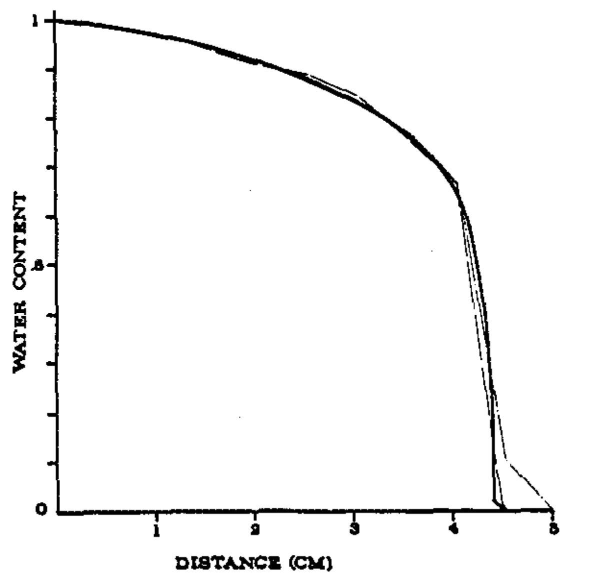

Fig. 14. Comparison of unmodified matrix formulation with diffusivity coefficients from (35) (dashed line) to improved finite difference approach (single-dot-dashed line).

sivity coefficients as determined by evaluating $D_i(\theta)$ at the parabolic mean value of soil water content at the endpoints of R_j. Comparison of these results (Figure 12) to the simulation determined by the modified finite difference approach reported by *Hayhoe* [1978] indicates a computational improvement over the modified finite difference scheme in predicting the location of the soil water wetting front. Figure 14 shows the simulated results from the unmodified capacitance matrix approach ($\alpha = 2$) and the modified finite difference method. Figure 15 shows the results from the unmodified capacitance matrix with the mean parabolic $D_i(\theta)$ parameters approach for finite element lengths of $\Delta t = 0.50$, 0.25, and 0.125 cm with the time step retained at $\Delta t = 0.1$ min.

CONCLUSIONS

An examination of the Galerkin method combined with the Crank-Nicolson time advance approximation to estimate unsaturated soil moisture transfer in a horizontal column indicates that the element capacitance matrix can be modified in order to approximate better the integration of water content over the finite element. Application of the modified capacitance matrix formulation to a normalized moisture transfer problem gives significant improvement in computational accuracy over the results obtained from the unmodified capacitance matrix formulation.

Numerical results from approximating a variable soil water diffusivity function by a quasi-constant value within each finite element for small intervals of time are presented. Five techniques of determining a diffusivity coefficient are evaluated for computational accuracy in predicting the soil water content profile in a horizontal soil water infiltration problem. The resulting moisture content profiles from both the modified and unmodified capacitance matrix formulations are compared to the known Philip's solution for each of the five quasi-constant diffusivity computational schemes. Of the techniques considered, the best results were achieved when utilizing the unmodified capacitance matrix approach along with values of diffusivity coefficients evaluated at the mean parabolic value of the state variable (water content) at the midpoint of each finite element.

When compared to the results from the improved finite difference computational scheme [*Hayhoe*, 1978], the results obtained herein indicate better prediction of the soil moisture wetting front.

Acknowledgment. The work reported on here was funded by the U.S. Army, Cold Region Research and Engineering Laboratory, Hanover, New Hampshire, contract DACA89-78-G-002.

REFERENCES

Bruch, J. C., Jr., and G. Zyvoloski, Solution of vertical unsaturated flow of soil water, *Soil Sci.*, *116*, 417–422, 1974.

Desai, C. S., *Elementary Finite Element Method*, Prentice-Hall, Englewood Cliffs, N. J., 1979.

Douglas, J., Jr., and T. Dupont, Galerkin methods for parabolic equations, *SIAM J. Numer. Anal.*, *7*, 575–626, 1970.

Guymon, G. L., and J. N. Luthin, A coupled heat and moisture transport model for Arctic soils, *Water Resour. Res.*, *10*(5), 995–1001, 1974.

Hayhoe, H. N., Study of relative efficiency of finite difference Galerkin techniques for modeling soil water transfer, *Water Resour. Res.*, *14*(1), 97–102, 1978.

Myers, G. E., *Analytical Methods in Conduction Heat Transfer*, McGraw-Hill, New York, 1971.

Neuman, S. P., R. A. Feddes, and E. Bresler, Finite element analysis of two-dimensional flow in soils considering water uptake by roots, 1, Theory, *Soil Sci. Soc. Amer. Proc.*, *39*, 1975.

Philip, J. R., and J. H. Knight, On solving the unsaturated flow equation, 3, New quasi-analytic technique, *Soil Sci.*, *117*, 1–13, 1974.

Price, H. S., J. C. Cavendish, and R. S. Varga, Numerical methods of higher-order accuracy for diffusion-convection equations, *Soc. Petrol. Eng.*, *243*, 293–303, 1968.

Reichardt, K., D. R. Nielsen, and J. W. Biggar, Scaling of horizontal infiltration into homogeneous soils, *Soil Sci. Soc. Amer. Proc.*, *36*, 241–245, 1972.

Yoon, Y. S., and W. W.-G. Yeh, The Galerkin method for nonlinear parabolic equations of unsteady groundwater flow, *Water Resour. Res.*, *11*(5), 751–754, 1975.

(Received September 10, 1979;
revised March 3, 1980;
accepted March 12, 1980.)